Low-energy pion-nucleon scattering

W. R. Gibbs and Li Ai

Department of Physics, New Mexico State University, Las Cruces, New Mexico 88003

W. B. Kaufmann

Department of Physics and Astronomy, Arizona State University, Tempe, Arizona 85287

An analysis of low-energy charged pion-nucleon data from recent $\pi^\pm p$ experiments is presented. From the scattering lengths and the Goldberger-Miyazawa-Oehme (GMO) sum rule we find a value of the pion-nucleon coupling constant of $f^2 = 0.0756 \pm 0.0007$. We also find, contrary to most previous analyses, that the scattering volumes for the P_{31} and P_{13} partial waves are equal, within errors, corresponding to a symmetry found in the Hamiltonian of many theories. For the potential models used, the amplitudes are extrapolated into the subthreshold region to estimate the value of the Σ term. Off-shell amplitudes are also provided. [S0556-2813(98)01302-8]

I. INTRODUCTION

The pion-nucleon interaction has been a fruitful source of knowledge of the strong interaction. The properties of the baryon resonances produced in pion-nucleon collisions give strong support for the quark model. The subthreshold amplitude is related to the value of the pion-nucleon Σ term which constrains models of nucleon structure. The pion-nucleon coupling constant provides fundamental input for the calculation of nuclear forces. Beyond these surface features lie more subtle indications of the nature of the strong interaction.

We model the dynamics of this interaction by a coupled-channel Klein-Gordon equation whose potential is assumed to be the fourth component of a Lorentz vector. There are several advantages to this approach.

First, unitarity, Coulomb corrections, multichannel effects, and hadronic mass splittings may be included in a natural way. Next, by solving the Klein-Gordon equation at the appropriate kinematical point, any observable can be calculated, even in the subthreshold region. This is especially easy in the case of the s-wave scattering with an exponential potential, for which an analytical result is available.

By using such a model we are presented with an alternative approach to such quantities as the Σ term. While the value of the Σ term may well be more accurately determined by dispersion relations, by looking at it from the point of view of a potential theory the structure of the system is perhaps better revealed in the sense that the behavior of the subthreshold amplitude is directly related to the shape of the potential (and presumably to the distribution of the constituents of the pion and nucleon).

A more subtle advantage is that models which take a broader view of the system, including higher energy data, have the problem that the model must be valid over the entire range. In this way the low-energy parameters have been largely determined by the data at high energies and the assumed dependence of the model for the low-energy behavior. Thus such features as the singularities in the scattering amplitude due to cuts coming from the range of the interaction

depend almost entirely on the model assumptions. In the present technique, which does not claim to be a theory of the system, the low-energy regime can be investigated without recourse to data at higher energies. Finally, solutions in coordinate space allow us to develop an intuitive picture of the spatial structure of the interacting pion-nucleon system.

Our Klein-Gordon model also has several drawbacks: The model is purely phenomenological at the hadronic level. Because it is a model based on static potentials, virtual particle production and annihilation and retardation effects are not explicitly included. As with all potential models, effects of crossing symmetry must be inserted. Because of the efficiency of the Jost calculation of the s-wave amplitude for the exponential potential (and the rapid cutoff properties of the Gaussian potential in r space) we are able to incorporate (in a controlled approximation) the crossing symmetry condition that the isovector amplitude must vanish at $s=u$ into the fitting procedure. The relativistic effect in the center-of-mass motion is taken into account only approximately. Because we describe only low-energy phenomena, we believe that these defects are outweighed by the model's strengths.

In a previous paper [1] we presented results bearing on the breaking of isospin using the same technique applied here [2] with a selection of five different forms of potential. On examining the phase shifts produced outside the range of the fit it was noticed that the prediction was much better for two of the models, sums of local Yukawa and exponential potentials for each partial wave. From fitting the data from 30 to 50 MeV these two models were able to predict the existence of the 33 resonance, and indeed the position of the resonance to within about 10% in kinetic energy. Thus it seemed reasonable to extend the analysis to somewhat higher energy with one (or both) of these two models.

The Yukawa potential has the advantage that it naturally represents particle exchanges. As will be discussed in Sec. III, the Klein-Gordon equation contains a term which is quadratic in the potential. For a Yukawa potential, such a term is singular ($\propto 1/r^2$). While solutions of this equation are obtainable, the result would seem to be more physical if a cutoff is introduced to soften the potential at small values of r (per-

haps due to the intrinsic size the of quark-pion system). For an analysis employing particle exchange (hence approximately related to Yukawa potentials) see the recent work of Timmermans [3].

One goal of this article is the representation of the pion-nucleon interaction in a simple and transparent manner. The exponential potential lends itself to that end without introducing a singular potential. Another advantage of the exponential form is that it might better represent the interaction of the pion with quark distributions within the nucleon. (The density calculated from a bound-state solution of a wave equation with a $1/r$ potential is exponential, as in the hydrogen atom and a three body system tends to follow the same density [4].) We have also made a short study utilizing the Gaussian potential, even though it is not considered to have a strong physical basis, to estimate which results are sensitive to the form of the potential (see Sec. V H).

The article is organized as follows. Section II summarizes our choice of elastic-scattering data sets and briefly discusses their consistency. Section III reviews Jost's method for determining the s-wave amplitude for sums of exponential potentials. Our method of evaluation of the subthreshold amplitudes is described in Sec. IV. Section V begins by presenting numerical values of the potential parameters determined from a fit to the data. This is followed by subsections which present the consequences of the fit, such as the phase shifts, scattering lengths, coupling constant, σ term, off-shell amplitudes, partial integrated elastic cross section, and polarization asymmetry. The results are summarized in Sec. VI.

II. DATA

The data sets that we have considered come from, for the most part, experiments dedicated to the measurement of pion-nucleon scattering. We have excluded experiments which have not been published or which had the measurement of pion-nucleon scattering as a secondary goal. The sets used are as follows:

Sigg. The one atomic measurement by Sigg *et al.* [5] is very important in determining the low-energy behavior of the s-wave amplitudes. It alone fixes, to large extent, the scattering length of the $\pi^- $-$p$ system. We found that predictions of this scattering length from our fits to scattering data were always near to their value and, when included, the fit adapted itself easily to the value and usually fit it with a very small χ^2. Thus we see no reason to question the validity of this point and have used it in all of the analyses discussed below.

Brack. The data from Brack *et al.* [6–8] seem to be of high quality. The smallest errors are (in general) those quoted in this work, from which we have used 61 data points for scattering of π^+ and π^- at 29.4, 45.0, 66.8, and 86.8 MeV.

Frank. The data from Frank *et al.* [9] were the first modern data to be published contradicting the Bertin *et al.* [10] data. This work contains 166 data points for scattering of π^+ and π^- at 29.4, 49.5, and 69.6 MeV.

Auld. The data of Auld *et al.* [11] are somewhat old now and have large error bars but are generally consistent with
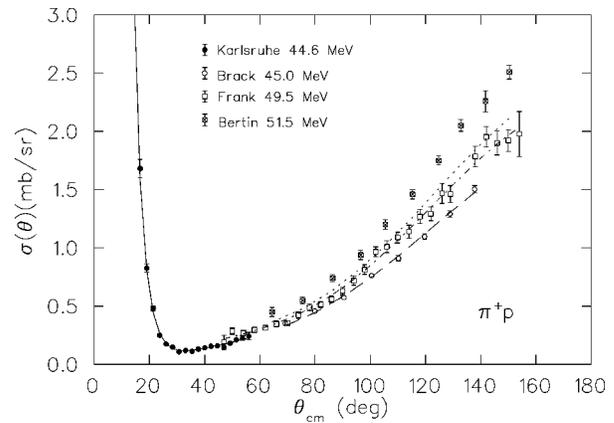

FIG. 1. Cross sections from π^+ proton scattering around 50 MeV. The Bertin data would agree with the prediction given by the dotted curve if they were consistent with the other data sets. The solid, long dash and dash-dot curves come from our fit and correspond to the Karlsruhe, Brack, and Frank data sets.

the modern data. These data contain 11 points for scattering of π^+ at 47.9 MeV.

Ritchie. The data from Ritchie *et al.* [12] consist of 28 points of back-angle positive pion scattering at 65.0, 72.5, and 80.0 MeV. We have found, as did Timmermans [3], that the normalization seems to be flawed in this data. We have floated the normalization of the lowest energy data set. (This data is from a secondary experiment.)

Wiedner. The data of Wiedner *et al.* [13] represent the first to appear in print from PSI (Paul Scherrer Institut). This set consists of π^+ and π^- scattering at 54.3 MeV. Our fit indicates that the cross sections for the negative pion data are too high by about 14%.

Joram I. The first paper of Joram *et al.* [14] presents data in the important Coulomb-nuclear interference region for π^+ and π^- at 32.20 and 44.60 MeV. The set contains 80 data points and seems to be consistent with the rest of the data base.

Joram II. The data in the second paper of Joram *et al.* [15] present larger angle cross sections of π^+ and π^- at 32.3, 44.6, and 68.6 MeV. The authors made single-energy fits to the data in the experimental paper. For the π^+ at 32.3 MeV the best χ^2/N that they obtained, in combination with other data at this energy, was 121/58, while for the π^+ at 44.6 MeV the best was 95.6/46. It was pointed out in Ref. [16] that the scattering lengths obtained from these single-energy fits lead to values of the πNN coupling constant outside of an acceptable range. We have not included these two data sets in our fit. We also have dropped the 53.42 degree point in the π^+ data at 68.6 MeV which is completely out of line with the rest of the data. This leaves 32 data points in this set.

The data of Bertin *et al.* [10] were not included in the general fits since they (or at least their normalizations) seem to be inconsistent with the modern data. In order to make contact with previous analyses and get some feeling for the impact of the data sets, we make fits using the Bertin data as the only π^+ data and the full modern π^- data set described above. Figure 1 shows the π^+ data around 50 MeV compared with one of our fits illustrating the apparent discrepancy.

III. SOLUTIONS FOR THE AMPLITUDES: JOST REPRESENTATION

At low energies and for each partial wave, the $\pi^+ p$ elastic process is described by a single-channel Klein-Gordon (KG) equation. The $\pi^- p$ elastic and charge-exchange scattering are described by a two-channel KG equation. That the effect of the (π^-, γ) reaction on the hadronic channels may be ignored was justified in Ref. [2] where this procedure is discussed in detail.

In fitting the data, we solve the KG equation by standard numerical procedures. The potential V is included in the KG equation through the substitution $\omega \rightarrow \omega - V$, where ω is the center-of-mass energy of the pion (actually the reduced energy in the fits); i.e., for both electrostatic and strong interactions, V is taken to be the fourth component of a Lorentz four-vector. The resulting equation is

$$(\nabla^2 + k^2 - 2\omega V + V^2)\psi = 0, \tag{1}$$

where k is the center-of-mass momentum.

However, there are several calculations that we would like to make which include only the strong interaction [the σ term, the isovector s-wave amplitude at the Cheng-Dashen (CD) point, and the off-shell amplitudes] for which the Coulomb force is not included. In this case it is very convenient to use (for the s wave) the expressions developed by Jost [17].

We now give a brief outline of the method and its extension to the off-shell case. Our potential contains (at most) two terms of exponential form. Since the potential appears linearly and quadratically in the KG equation, a two-term basic potential leads to an effective Schrödinger equation with a five-term potential.

Consider the solution of the Schrödinger equation for a sum of exponential potentials

$$V(r) = \sum_{j=1}^{N} \lambda_j e^{-\mu_j r}. \tag{2}$$

Jost [17] writes the solution for the s wave, $f(k,r)$, as

$$f(k,r) = e^{-ikr} \sum_{\alpha} C_\alpha(k) e^{-m_\alpha r}, \tag{3}$$

where the subscript α is a compound quantity consisting of a set of N integers. For example, for a three-term potential,

$$\alpha \equiv [j,k,l], \quad j,k,l = 0,1,2\cdots. \tag{4}$$

The coefficients $C_\alpha(k)$ are given by the recursion relation

$$C_{[j,k,l]}(k) = \frac{\lambda_1 C_{[j-1,k,l]} + \lambda_2 C_{[j,k-1,l]} + \lambda_3 C_{[j,k,l-1]}}{m_\alpha(m_\alpha + 2ik)}, \tag{5}$$

where

$$m_\alpha \equiv m_{[j,k,l]} \equiv j\mu_1 + k\mu_2 + l\mu_3. \tag{6}$$

The recursion is started with

$$C_{[0,0,0]} = 1, \quad C_{[-1,k,l]} = C_{[j,-1,l]} = C_{[j,k,-1]} = 0 \tag{7}$$

and is built up by first computing all coefficients with the sum of indices equal to one, then two, etc., with no negative index.

The solution with the proper boundary conditions at the origin with an incoming spherical wave and with unit amplitude at infinity is

$$\psi(k,r) = -\frac{f(k,r) - S(k)f(-k,r)}{2ikr}, \tag{8}$$

where

$$S(k) = \frac{f(k,0)}{f(-k,0)}. \tag{9}$$

These expressions can be used to calculate the values of the S matrix for any value of k. We shall be interested in purely imaginary values for the calculation of the s-wave contribution to the Σ term.

In order to calculate the off-shell amplitude we consider the wave function for real (positive) values of k. In this case we can write (for real λ_j)

$$f(-k,r) = f^*(k,r) \tag{10}$$

with $S = e^{2i\delta}$ and $f(k,0) = e^{i\delta}\beta$, where β is real and positive. We can now write the wave function [Eq. (8)] as

$$\psi(k,r) = -\frac{e^{i\delta}}{2ikr}\left[e^{-i\delta}e^{-ikr}\sum_{\alpha} C_\alpha(k)e^{-m_\alpha r} - e^{i\delta}e^{ikr} \right.$$
$$\left. \times \sum_{\alpha} C_\alpha(-k)e^{-m_\alpha r} \right]. \tag{11}$$

The s-wave off-shell amplitude is defined by

$$F_0(k,q) \equiv \int dr\, r^2 j_0(qr) V(r)\psi(k,r) \tag{12}$$

and we find

$$F_0(k,q) = \frac{e^{i\delta}}{k} Im\left[e^{-i\delta}\sum_{\alpha} C_\alpha(k) \right.$$
$$\left. \times \sum_{j} \frac{\lambda_j}{(m_\alpha + \mu_j)^2 + q^2 - k^2 + 2ik(m_\alpha + \mu_j)} \right]. \tag{13}$$

This function is evaluated in Sec. V E.

IV. SUBTHRESHOLD EXTRAPOLATION

The subthreshold regime, the region below the elastic threshold, is of interest in studies of chiral-symmetry breaking, a measure of which is the Σ term. On-shell subthreshold amplitudes have been evaluated over the years by the use of dispersion relations [18–22]. It is interesting to compare those results with the values given by the KG equation.

A. Dispersion relations

Because the "experimental" Σ term is defined at the unphysical Cheng-Dashen [23] point ($s=m^2$, $t=2\mu^2$), any determination of it is, to a degree, model or theory dependent. s-channel and u-channel data exists only for negative t, therefore fixed-t dispersion relations must either rely on the rapid convergence of the partial-wave series outside of the physical region at $t=2\mu^2$ as in Cheng and Dashen's method or must use additional techniques (such as dispersion relations at fixed ν) to extend the amplitudes to $t=2\mu^2$. This extrapolation is complicated by the presence of the crossed reaction $\pi\pi \to N\bar{N}$ which produces a nearby branch cut in the t channel beginning at $t=4\mu^2$. Some knowledge of the effect of this cut is obtained indirectly from $\pi\pi$ elastic scattering, but this analysis is, to an extent, model dependent. Some formulations of the dispersion relation approach rely heavily on very accurate knowledge of the p-wave scattering volume [22] when, in fact, the Σ term is dominated by the s-wave amplitude [24,25].

Interior dispersion relations (IDR's) [21] and hyperbolic dispersion relations [20] have also been used to determine the Σ term. In these cases, the curves along which the dispersion relations are written may be chosen to pass directly through the CD point. However, these dispersion relations involve integrals over the entire t-channel cut, a long portion of which is unphysical ($4\mu^2 \lesssim t < 4m^2$). In this case, the entire t-channel dispersion integral (the "discrepancy function") must be determined and extrapolated to the CD point. Thus, even in the classic dispersion-theory determination of the Σ term, some model dependence is present.

It is instructive to compare the relative contributions of the s and p waves to the nonflip pole-subtracted amplitude $\widetilde{G}^+$ which is real in this region and, as we shall show in the next section, is proportional to Σ at the CD point. To this end we have performed the partial-wave projections of $\widetilde{G}^+$ as computed from the subthreshold polynomial expansion in $\nu=(s-u)/4m$ and t from Höhler et al. [28]. For purposes of illustration we plot $\widetilde{G}^+$ vs ν along a curve of constant path parameter $a=-\phi(s,t)/t^2$, where $\phi(s,t)=t[su-(m^2-\mu^2)^2]$ is the Kibble function, which vanishes on the boundary of the physical region. The parameter a is fixed at the value $-m^2+\mu^2/2$. This path has the advantage that it passes through both the s-channel threshold ($\nu=\mu$) and the CD point (at which $\nu=0$). It also arrives at the CD point tangent to a curve of constant t as was specified in the paper of Cheng and Dashen. (This is the path used in IDR calculations.) For comparison, the s and $s+p$ wave partial-wave contributions to $\widetilde{G}^+$ are plotted along with the full amplitude in Fig. 2. The amplitudes have been multiplied by a factor so that they reduce to the Σ term at $\nu=0$. It is seen that the s wave contribution is similar to the full amplitude $\widetilde{G}^+$ between the CD point and threshold, becoming quite close at the CD point. Notice that the s and $s+p$ contributions cross slightly below the CD point, where $\cos\theta$ vanishes. This zero in $\cos\theta$ suppresses the p-wave contribution at the CD point [24]. The value of $\cos\theta$ at the CD point is

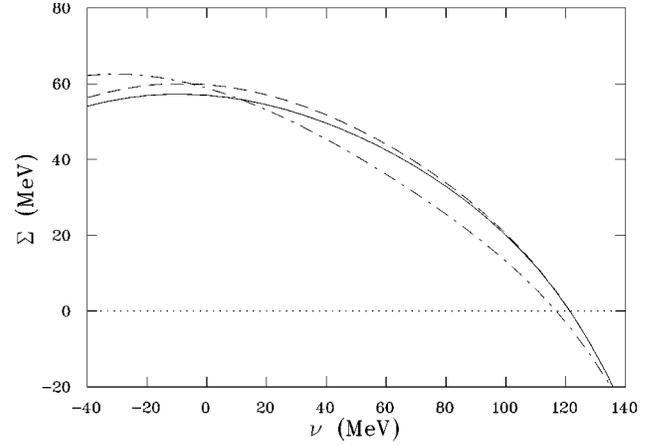$$\cos\theta = -\frac{\mu^2}{4m^2-\mu^2} \approx -\frac{1}{180}. \tag{14}$$

FIG. 2. Contributions to the Σ term for the s wave (dash-dot curve) the s and p waves (dashed curve) and the full amplitude (solid curve) from the polynomial expansion from Ref. [28]. From this graph the p wave is estimated to give a correction of $\sim +1$ MeV. The sum of all of the non-s-wave contributions gives ~ -1.5 MeV.

The value of t for which $\cos\theta$ is zero (for $\nu=0$) is approximately

$$t=2\mu^2\left(1-\frac{\mu^2}{4m^2}\right) \tag{15}$$

which differs from the value at the CD point by about 1/2 of one percent.

B. Klein-Gordon approach

In the present approach the subthreshold dependence is derived directly from the pion-nucleon data itself. The question of the validity of the function extracted then depends on the accuracy of the data and the suitability of the form used for the potential.

Many calculations use the Coulomb corrections developed by Tromborg et al. [26]. For our particular application, a coordinate-space coupled-channel calculation, it is more natural and self-consistent to include hadronic mass splittings explicitly, and include the Coulomb interaction through the use of a static Coulomb potential. Indeed, this is one of the advantages of our approach. Because the Coulomb is included as a potential, Coulomb-hadronic interference in computed to all orders. As a bonus, we can incorporate the finite hadronic size (a small correction). In some incarnations of our code we have included magnetic interactions (following Ref. [27]), but this is a very small effect at low energies. Higher-order QED effects such as such as crossed-photon exchange have been omitted. Another electromagnetic effect that we have considered is influence of the photoproduction channel on the elastic channels. This was shown to be negligible in an earlier article [2]. Finally, since we have included the Coulomb potential to all orders, one could directly solve the bound-state problem to directly obtain pionic atomic level shifts and widths.

While the amplitudes produced from the KG model do not automatically contain the full analyticity and crossing properties of the invariant amplitudes, much of the same

TABLE I. Ranges and strengths for the potential obtained from a fit to the data corresponding to line 13 in Table IV. The radii are calculated in the rms sense.

Partial Wave	α_1 (MeV/c)	λ_1 (MeV)	α_2 (MeV/c)	λ_2 (MeV)	R_1 (fm)	R_2 (fm)
S_3	722.9	898.9	487.8	-39.3	0.946	1.401
S_1	748.9	-1.5	310.5	-58.0	0.913	2.201
P_{33}	891.7	401.6	486.7	-1545.9	0.767	1.404
P_{13}	814.0	-5586.5	528.7	820.1	0.840	1.293
P_{31}	630.3	1806.3			1.084	
P_{11}	720.4	-3542.5			0.949	

physics can be included by considering that the source of the potential is the t-channel cut ($\pi\pi$ scattering and $\pi\pi \to N\bar{N}$). The potential can be written in terms of an integral over the discontinuity along the t axis as done in the case (for example) of the NN potential [29]

$$V(r) = \int_{4\mu^2}^{\infty} \rho(t) \frac{e^{-\sqrt{t}r}}{r} dt. \qquad (16)$$

Since a Yukawa potential can be written as an integral over an exponential form

$$\frac{e^{-\mu r}}{r} = \int_{\mu}^{\infty} e^{-xr} dx \qquad (17)$$

the πN potential can be expressed as a sum of exponential potentials.

From the definition of the non-spin-flip amplitude

$$G(s,t) = \sum [(2\ell+1)f_{\ell+} + \ell f_{\ell-}]P_\ell(x), \qquad (18)$$

and the projection of these partial waves from the invariant amplitudes $A(s,t)$ and $B(s,t)$ (see Ref. [30], Eq. (2.7) for example) we can write

$$16\pi s G^{(+)}(s,t) = [(W+m)^2 - \mu^2][A^{(+)}(s,t) + (W-m)B^{(+)}$$
$$\times (s,t)] + x[(W-m)^2 - \mu^2][-A^{(+)}(s,t)$$
$$+ (W+m)B^{(+)}(s,t)], \qquad (19)$$

where $W = \sqrt{s}$ and x ($=\cos\theta$) is a function of s and t. The same result is available from Eq. (A 2.32) of Ref. [18]. We omit the superscript $(+)$ for the next few equations for clarity. For $t = 2\mu^2$ the Born term contribution to B, $g^2[1/(m^2 - s) - 1/(m^2 - u)]$, becomes $-2g^2/(s - m^2)$.

If we define $\widetilde{B}(s,t)$ as the B amplitude with the pole term removed then

$$16\pi s G(s, 2\mu^2)$$

$$= [(W+m)^2 - \mu^2]\left[A(s, 2\mu^2) + (W-m)\widetilde{B}(s, 2\mu^2) \right.$$
$$\left. - \frac{2g^2}{W+m} \right] + x[(W-m)^2 - \mu^2]\left[-A(s, 2\mu^2) \right.$$
$$\left. + (W+m)\widetilde{B}(s, 2\mu^2) - \frac{2g^2}{W-m} \right] \qquad (20)$$

or

$$[(W+m)^2 - \mu^2]\left[A(s, 2\mu^2) + (W-m)\widetilde{B}(s, 2\mu^2) - \frac{2g^2}{W+m} \right]$$

$$= 16\pi s G(s, 2\mu^2) - \frac{2g^2\mu^2 x}{W-m} - x(W-m)^2$$

$$\times [-A(s, 2\mu^2) + (W+m)B(s, 2\mu^2)]$$

$$+ x\mu^2[-A(s, 2\mu^2) + (W+m)\widetilde{B}(s, 2\mu^2)]. \qquad (21)$$

Now define $\widetilde{G}(s, 2\mu^2) \equiv G(s, 2\mu^2) - \mu^2 g^2 x/8\pi s(W-m)$ to remove the pole from the P_{11} partial wave. The subtracted pole term should be evaluated with the fitted position and residue so that the pole is exactly removed from the P_{11} partial wave of $G(s, 2\mu^2)$. Then, at the CD point ($s = m^2$),

TABLE II. Ranges and strengths for the potential obtained from a fit to the data corresponding to line 14 in Table IV, as in Table I.

Partial Wave	α_1 (MeV/c)	λ_1 (MeV)	α_2 (MeV/c)	λ_2 (MeV)	R_1 (fm)	R_2 (fm)
S_3	715.8	858.9	462.3	-33.1	0.954	1.479
S_1	602.8	-19.6	311.7	-55.2	1.134	2.193
P_{33}	891.3	289.7	488.7	-1540.6	0.767	1.399
P_{13}	810.0	-5563.9	526.9	823.6	0.844	1.293
P_{31}	638.7	1931.7			1.070	
P_{11}	720.2	-3545.1			0.949	

TABLE III. Results of the study. χ^2 is separated into contributions from the individual data points and from the experimental normalization uncertainty. The fits were made including a contribution to the total χ^2 from Eq. (26) of $\Delta E_\Sigma = 10$ MeV. The line labeled PSI includes both the Wiedner and Joram data.

	χ^2/n (data)	χ^2/n (norm)	Σ (MeV)	a_3 (μ^{-1})	a_1 (μ^{-1})	f^2
Brack	64.66/62	9.88/10	42.86	-0.083	0.174	0.0751
+Frank	231.78/228	21.85/16	48.43	-0.085	0.174	0.0754
+Auld	243.28/239	23.20/17	48.59	-0.085	0.174	0.0754
+Ritchie	274.58/267	27.68/20	48.66	-0.085	0.174	0.0754
+Wiedner	316.27/306	33.09/22	50.01	-0.085	0.174	0.0754
+Joram I	432.67/386	35.42/26	48.90	-0.081	0.172	0.0743
+Joram II	497.93/417	42.01/30	53.59	-0.082	0.172	0.0745
Frank	144.15/167	4.56/6	48.34	-0.083	0.173	0.0749
PSI	153.49/151	8.33/10	67.45	-0.095	0.180	0.0785
Bertin+π^-	278.56/243	15.96/18	52.92	-0.105	0.183	0.0809

$$(4m^2 - \mu^2)\left[A(m^2, 2\mu^2) - \frac{g^2}{m} \right]$$

$$= 16\pi m^2 \widetilde{G}(m^2, 2\mu^2) + x_{CD}\mu^2[-A(m^2, 2\mu^2)$$

$$+ 2m\widetilde{B}(m^2, 2\mu^2)]. \qquad (22)$$

The last term is negligible at the CD point as we will show shortly. Thus, neglecting the factor $(1 - \mu^2/4m^2)$,

$$4\pi\widetilde{G}^{(+)}(m^2, 2\mu^2) = A^{(+)}(m^2, 2\mu^2) - \frac{g^2}{m} = \Sigma/f_\pi^2, \quad (23)$$

where $f_\pi = 93.2$ MeV is the pion decay constant. The equation corresponding to the second equal sign has been given many places (see [31], for example). The corrections to this expression of the order $(\mu/m)^4$ [32].

The ratio of the last two terms in Eq. (22) is approximately

$$x_{CD}\mu^2[-A + 2m\widetilde{B}]f_\pi^2/(4m^2\Sigma) \approx 0.002,$$

where we have used $A \approx g^2/m \approx 191$ GeV^{-1}, $2m\widetilde{B} \approx -311$ GeV^{-1}, $\Sigma \approx 0.060$ GeV, and $x_{CD} \approx -\mu^2/4m^2$. Thus we may safely ignore the last term in Eq. (22).

Thus, to a good approximation, the sigma term can then be evaluated as $\Sigma = 4\pi f_\pi^2 \widetilde{G}^{(+)}$, where $\widetilde{G}^{(+)}$ is evaluated at the CD point. We approximate $\widetilde{G}^{(+)}$ by s-channel isospin amplitudes $G^{(+)} = \frac{1}{3}(G^{1/2} + 2G^{3/2})$.

The CD point occurs at center-of-mass total pion energy, $\omega = \mu^2/2m \approx 0$; at this point, the effective potential $U = 2\omega V - V^2 \approx -V^2$ is attractive whatever the sign of V. Above threshold the cross term dominates, and U may be either positive or negative. We are particularly interested in the s-wave scattering amplitudes because, as discussed in the previous section, at the CD point $\cos\theta \approx 0$ and the p-wave contributions to the sigma term are suppressed. At threshold one of the s-wave amplitudes, $S_{1/2}$ is positive, and the other $S_{3/2}$ is negative. We define renormalized amplitudes by

$$\Sigma_I = 4\pi f_\pi^2 G_I^{(+)} \approx 4\pi f_\pi^2 S_I \approx 553 S_I, \qquad (24)$$

where S_I are the s-wave scattering amplitudes in fm, and $I = \frac{1}{2}, \frac{3}{2}$. When evaluated at the CD point $\Sigma = \frac{1}{3}(\Sigma_{1/2} + 2\Sigma_{3/2})$ is the σ term. As ω passes below threshold ($\omega = \mu$) these two amplitudes will keep their signs (they are real in this region) but at $\omega = 0$ they must be of the same sign (and positive) because the square term now dominates (unless the squared potential is strong enough that there is a bound state).

In the low-energy physical region there is a correlation between the range and strength of each potential; i.e., two fits are, to lowest order, comparable if the volume integrals of the potentials are equal. However, in the subthreshold region near the CD point the V^2 term dominates $2\omega V$ ($\omega \approx 0$); the correlation no longer holds. Therefore to determine the amplitude near the CD point with our model, the strength and range of the potentials must be independently determined. We believe that the available data is sufficiently accurate that this determination can be made, at least approximately.

Since $A^{(-)}(m^2, 2\mu^2) = 0$ and the Born term is zero at the same point, we find

$$G^{(-)}(m^2, 2\mu^2) \approx 0, \qquad (25)$$

where the zero is of order $(\mu^2/4m^2)^2$ times a typical amplitude. Since the isovector amplitude $G^{(-)}(m^2, 2\mu^2)$ vanishes, it follows that the isovector combination $\Sigma^- = \Sigma_{1/2} - \Sigma_{3/2}$ should vanish (assuming s-wave dominance) at the CD point so that the two amplitudes defined in Eq. (24) should cross at that point. This vanishing is not automatic in the KG model, which does not have $s \leftrightarrow u$ crossing built in. In performing a number of fits without this requirement we found that $\Sigma_{1/2}$ and $\Sigma_{3/2}$ do indeed naturally cross near $\nu = 0$. However, the isovector amplitude varied between 10 and 100 MeV at $\nu = 0$. Even so, we obtained stable values for the scattering lengths while values of the Σ term varied from 33 to 100 MeV.

Using the Jost technique described in Sec. III we evaluated Σ^- at the CD point at each step of the fit. By including a contribution of

$$\left(\frac{\Sigma_{3/2} - \Sigma_{1/2}}{\Delta E_\Sigma} \right)^2 \qquad (26)$$

TABLE IV. Results of the study. The fits were made including a contribution to the total χ^2 from Eq. (26) of $\Delta E_\Sigma = 1$.

		χ^2/N (data)	χ^2/N (norm)	Σ (MeV)	a_3 (μ^{-1})	a_1 (μ^{-1})	f^2
1	Brack	66.37/62	9.70/10	50.51	-0.082	0.174	0.0749
2		65.09/62	10.52/10	45.53	-0.083	0.174	0.0751
3	+Frank	234.69/228	21.56/16	50.77	-0.085	0.175	0.0756
4		230.63/228	22.63/16	46.32	-0.086	0.174	0.0756
5	+Auld	245.35/239	22.88/17	50.76	-0.085	0.175	0.0762
6		242.43/239	23.46/17	46.32	-0.086	0.175	0.0758
7	+Ritchie	276.50/267	28.21/20	50.79	-0.086	0.175	0.0758
8		273.59/267	27.94/20	45.36	-0.086	0.174	0.0756
9	+Wiedner	317.40/306	35.12/22	49.86	-0.086	0.176	0.0760
10		315.21/306	33.12/22	45.53	-0.087	0.175	0.0760
11	+Joram I	431.89/386	37.97/26	48.98	-0.083	0.174	0.0751
12		432.83/386	35.58/26	45.14	-0.083	0.173	0.0749
13	+Joram II	495.96/417	44.57/30	49.22	-0.084	0.174	0.0753
14		500.67/417	42.64/30	45.99	-0.085	0.173	0.0753
15	Frank	139.07/167	4.41/6	48.67	-0.083	0.174	0.0749
16		139.27/167	4.71/6	46.51	-0.083	0.174	0.0749
17	PSI	153.32/151	8.38/10	65.17	-0.095	0.180	0.0785
18	Bertin+π^-	271.40/243	17.47/18	50.68	-0.103	0.184	0.0818
19		273.53/243	15.87/18	48.94	-0.105	0.184	0.0812

to the χ^2 it was possible to force the vanishing of $\Sigma^-(\nu = 0)$ to a reasonable degree of accuracy. The result is that the value of the Σ term obtained is much more stable. See Ref. [33] for a related discussion of subthreshold constraints on potential models.

V. RESULTS OF THE FIT

The form of the potential for each partial wave was taken as

$$V(r) = \lambda_1 e^{-\alpha_1 r} + \lambda_2 e^{-\alpha_2 r}. \quad (27)$$

The parameters in these potentials were determined by fitting to the data set by minimizing a χ^2 function. The total χ^2 was the sum of (1) the χ^2 from the data set (including the pionic atom point), (2) the χ^2 from the normalizations (defined as the square of the difference of the normalization from unity divided by the quoted experimental estimate of the error), and (3) the χ^2 from Eq. (26).

The second term was not needed for two of the partial waves. As an example of the values obtained, the strengths and ranges are given in Tables I and II for the cases of lines 13 and 14 of Table IV. We see that the ranges corresponding to the dominant strengths mostly have values from 500–900 MeV/c. An exception is the partial wave S_{11} where the value is ~ 310 MeV/c, barely above 2 pion masses, the minimum acceptable value without creating an anomalous threshold. That such a long (spatial) range is needed to fit this partial wave was noted by Ref. [34].

We have tested individual data sets to see their influence on the fits. The results presented in Tables III and IV show the effect of adding, one by one, the data sets in the order

shown. Below the solid lines are fits to single groups of data. The second line that appears in most entries of Table IV corresponds to a second fit which gives an idea of the uniqueness of the fits.

A. Phase shifts and low-energy parameters

Figures 3–6 show the phase shifts resulting from the fit 14 of Table IV.

We obtain for the isoscalar and isovector scattering lengths

$$b_0 = (2a_3 + a_1)/3 = 0.001 \pm 0.003 \quad \mu^{-1} \quad (28)$$

and

$$b_1 = (a_3 - a_1)/3 = -0.086 \pm 0.003 \quad \mu^{-1}, \quad (29)$$

in reasonable agreement with the values obtained by Sigg et al. [5]. A recent QCD calculation by Bernard et al. [35] gives $-0.096\mu^{-1} \leq b_1 \leq -0.088\mu^{-1}$ with which we are in marginal agreement.

The Chew-Low theory [36] predicts the values of the scattering volumes for all of the p waves. For the P_{33} the prediction is $0.191\mu^{-3}$ (using $f^2 = 0.0765$), in reasonable agreement with the values obtained.

An interesting feature of the P_{31} and P_{13} partial wave phase shifts (Fig. 4) is that they are very nearly equal at low energies, becoming essentially identical at threshold (Table V). Above 20 MeV in kinetic energy the curves separate. The Chew-Low theory predicts that these partial waves are always equal. Improved models [37,38] give different magnitudes for these scattering volumes, but the symmetry of the Hamiltonian requires that they be equal.
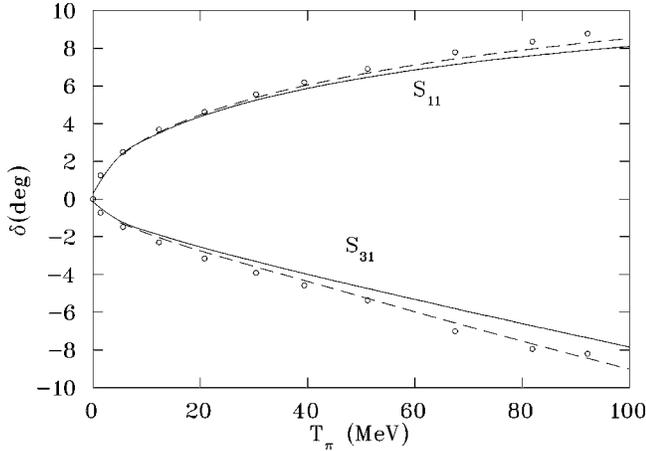
FIG. 3. *s*-wave phase shifts. The solid curve is the result of the present work for case 41 of Table IV. The circles are the results of the KH80 solutions and the dashed line is from SM95.

It is not clear how fundamental this symmetry should be considered to be, and thus on what level we should expect it to hold. It has been known for some time that this spin-isospin symmetry holds in the Skyrmion model [39]. Recently it has been shown [40] that the relations among partial waves of the Skyrmion model hold more generally in the large $1/N_c$ expansion of QCD. Since the predictions are for infinitely massive nucleons the symmetry might well be expected to be broken above threshold where recoil effects become important.

Comparisons with data have always shown this symmetry *not* to be satisfied in nature, but we find that it *is* satisfied within the errors. We find for both scattering volumes $-0.028 \pm 0.003 \ \mu^{-3}$.

Figure 4 shows that the KH80 phase shifts [41] follow our curve for values above 50 MeV but deviate at 20, 30, 40, and 50 MeV, just at the Bertin energies. Table V shows that, indeed, the analysis using the Bertin data results in a P_{31} scattering volume considerably larger than the P_{13}. For the P_{33} phase shift (Fig. 6) we note that the data fit in the region of 30 to 86 MeV give the behavior of this resonant phase shift with a reasonable accuracy.

The P_{11} phase shift (Fig. 5) is seen to have a negative excursion at low energies and to cross zero around 140 MeV,
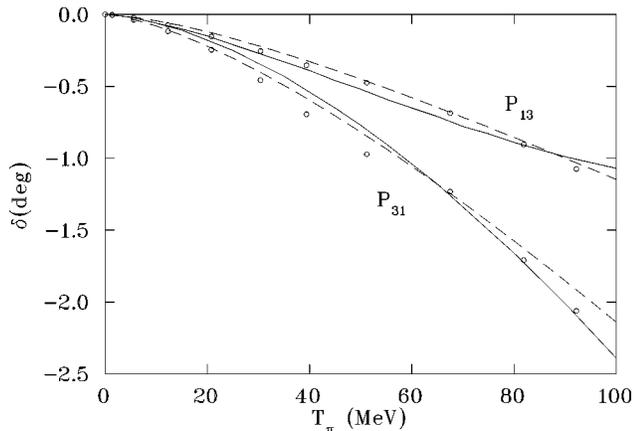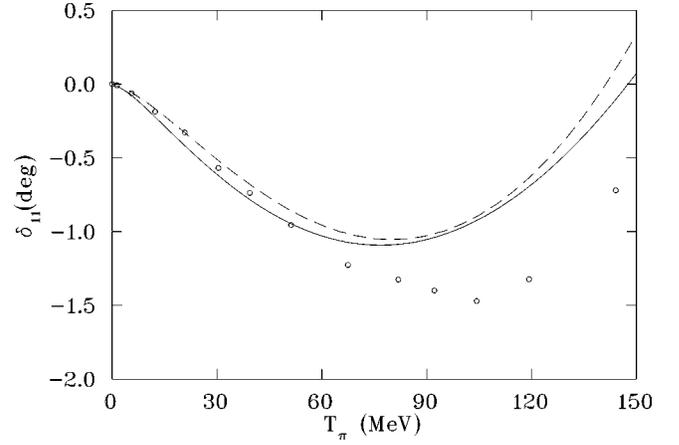

FIG. 5. P_{11} wave phase shifts. The curves and symbols have the same meaning as in Fig. 3.

as has been typical in previous fits. However, in the present case, it is the low-energy data alone which find this behavior, rather remarkable in view of the small size of the amplitude.

B. Isospin breaking

We have calculated the prediction for the charge-exchange amplitude for each of the fits shown in Table IV in the same manner as discussed in Ref. [1].

The charge-exchange data fit are the same as before [42–44]. Note that the fit to this data is direct, it requires no model and could have been done with a simple polynomial. The normalization of the data is constrained with the use of the TRIUMF data [43,44]. While these data provide only limited angular information, they give a relatively accurate value for the integrated charge-exchange cross section and thus provide an important normalization constraint.

While in the previous work [1] we demonstrated a small dependence on the model used for the charged pion scattering, here we show (Fig. 7) a comparison of the charge-exchange amplitudes determined directly from the measurements (the same as in [1]) with the predictions of six of the fits from Table IV (1, 2, 11, 12, 15, and 16). As can be seen, the variations among the data sets is small compared with the discrepancy.
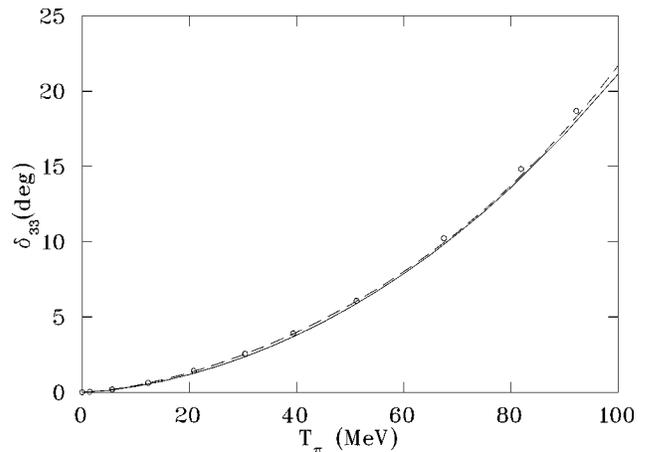

FIG. 4. P_{31} and P_{13} wave phase shifts. The curves and symbols have the same meaning as in Fig. 3.

FIG. 6. P_{33} wave phase shifts. The curves and symbols have the same meaning as in Fig. 3.

TABLE V. Slope parameters (μ^{-3}) for the s waves (B_3 and B_1) and scattering volumes (μ^{-3}) from the fit. The quantity B is defined by the relation $\mathrm{Re}(F)=a+Bq^2+\cdots$ for the s waves. The entries in this table correspond to those in Table IV.

		B_3	B_1	P_{33}	P_{13}	P_{31}	P_{11}
1	Brack	−0.050	−0.068	0.181	−0.031	−0.029	−0.102
2		−0.049	−0.064	0.178	−0.031	−0.031	−0.098
3	+Frank	−0.050	−0.068	0.179	−0.027	−0.028	−0.104
4		−0.049	−0.065	0.176	−0.027	−0.029	−0.102
5	+Auld	−0.050	−0.068	0.179	−0.027	−0.027	−0.105
6		−0.049	−0.065	0.176	−0.027	−0.028	−0.102
7	+Ritchie	−0.050	−0.068	0.180	−0.027	−0.026	−0.106
8		−0.048	−0.064	0.177	−0.028	−0.028	−0.102
9	+Wiedner	−0.050	−0.073	0.178	−0.026	−0.029	−0.108
10		−0.048	−0.064	0.177	−0.027	−0.028	−0.102
11	+Joram I	−0.049	−0.071	0.179	−0.027	−0.028	−0.108
12		−0.048	−0.063	0.177	−0.028	−0.028	−0.103
13	+Joram II	−0.049	−0.071	0.178	−0.025	−0.028	−0.106
14		−0.049	−0.064	0.176	−0.026	−0.027	−0.102
15	Frank	−0.049	−0.071	0.169	−0.015	−0.025	−0.109
16		−0.049	−0.065	0.168	−0.014	−0.025	−0.108
17	PSI	−0.055	−0.083	0.183	−0.027	+0.392	−0.119
18	Bertin+π^-	−0.049	−0.076	0.178	−0.023	−0.033	−0.100
19		−0.049	−0.070	0.177	−0.024	−0.034	−0.094

It is worthwhile to discuss the size of the result. It is possible to obtain a large *fraction* for the breaking because of the smallness of the basic amplitude itself. Let us compare with the NN case. If we assume that the *potential* causing the breaking is the same for πN and NN (as happens to be the case for $\rho\omega$ mixing [45]) then (in Born approximation) the breaking amplitude should be smaller for the pion-nucleon case by a factor of the ratio of the pion mass to the nucleon mass (about 0.14). However, a typical pion-nucleon amplitude at low energy (0.1–0.2 fm) is a factor of 100 smaller than a typical nucleon-nucleon amplitude (15–20 fm). Hence the percentage of the breaking should be around 10 times larger in the pion case compared to the nucleon-nucleon

case. The breaking amplitude observed here (~ 0.012 fm) would correspond to a breaking in NN case of around 0.1 fm which is too small to be observed at the present time. The predictions with the Bertin data, from line 19 in Table IV (not shown in the figure) agree with the measured charge exchange (as previously observed [1]).

A possible explanation has been advanced by Piekarewicz [46] for this breaking in terms of the difference of π^0 pion-nucleon coupling constants for the neutron and proton. This explanation would put the breaking entirely in the charge-exchange channel or the a_7 coefficient in the notation of Ref. [47].

C. The pion-nucleon coupling constant

The Goldberger-Miyazawa-Oehme (GMO) [48] sum rule provides a useful relation [49] between the isovector combination of the πN scattering lengths and the πNN coupling constant f^2. This sum rule is obtained from a forward dispersion relation for the invariant amplitude C^- evaluated at $\omega_{\mathrm{LAB}}=\mu$ [18].

$$4\pi\frac{m+\mu}{3m\mu}(a_1-a_3)=\frac{8\pi f^2}{\mu^2-\omega_B^2}+4\pi J,\qquad(30)$$

where

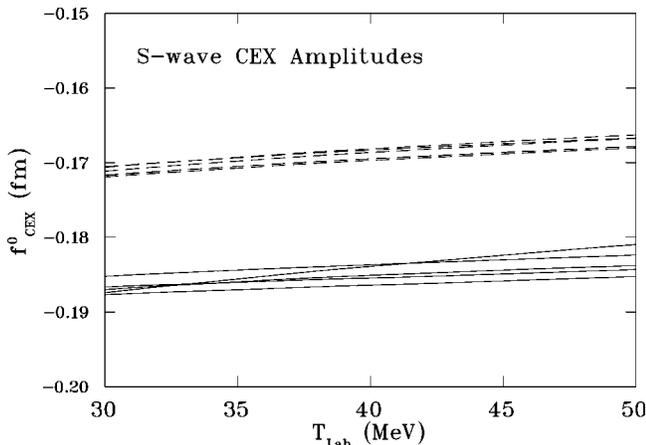$$J=\frac{1}{2\pi^2}\int_0^\infty\frac{\sigma^-(k)}{\omega(k)}dk.\qquad(31)$$

FIG. 7. s-wave amplitudes for pion-nucleon charge exchange, measured (solid lines) and predicted by isospin from the present fit (dotted lines).

In this expression k is the incident pion laboratory mo-

mentum and $\omega_B = -\mu^2/2m$. The isospin-odd total cross section is defined by $\sigma^- = 12(\sigma_- - \sigma_+)$, where $\sigma_\pm = \sigma_T(\pi^\pm p)$.

To evaluate J we have used the SM95 [50] phase shift analysis for $k < 2$ GeV/c, our own parametrization for 2 GeV/$c < k < 4$ GeV/c (a fit to total cross section data taken from the Review of Particle Properties [51]), and a Regge fit for 4 GeV/$c < k < 240$ GeV/c taken from the same source. If the integral is truncated above 240 GeV/c, the resulting value is $J = (-1.308 + 0.068 + 0.157)$ mb $= -1.081 \pm 0.005$ mb where the contribution from each momentum interval is shown. If we assume that the Regge fit is valid to infinite momenta, the contribution to J coming from above 240 GeV/c is 0.030 mb, which leads to $J = -1.051$ mb, in excellent agreement with the value used in the recent work of Arndt *et al.* [52]. For the following discussion we will use this value. The reader who wishes to use another value of J can shift our value of f^2 accordingly. This value can be compared with $J = -1.072$ mb obtained by Ref. [49] and $J = -1.077$ mb quoted in Ref. [49] from an unpublished preprint by Koch. Locher, Sainio [53] concluded that the uncertainty in J leads to a 1% error in f^2. Thus, we have the simple formula for f^2 (a_1 and a_3 in pion mass units)

$$f^2 = 0.0261 + 0.1904(a_1 - a_3). \qquad (32)$$

Some of the results of our fits to the low-energy $\pi^\pm p$ elastic scattering data are shown in Tables III and IV. The resulting average value of the coupling constant is $f^2 = 0.0756 \pm 0.0007$ where the error quoted includes only our fitting error determined from the variation among data sets.

The values for the scattering lengths advocated by SM95, $a_3 = -0.087 \mu^{-1}$ and $a_1 = 0.175 \mu^{-1}$, lead to $f^2 = 0.0760$ when used in our relation. Arndt *et al.* [54] quote a value of $f^2 = 0.076 \pm 0.001$ while Markopoulou-Kalamara and Bugg [55] found $f^2 = 0.0771 \pm 0.0014$. Timmermans quotes a preliminary value from his πN analysis [3] of $f^2 = 0.0741 \pm 0.0008$ (statistical error only).

Thus recent analyses of the charged pion coupling constant from pion-nucleon scattering seem to be in moderately good agreement. It is very interesting to know if this value is consistent with that obtained from the nucleon-nucleon interaction since that comparison serves as a check on our theory of the strong interaction.

The Nijmegen group [56] found $f^2 = 0.0748 \pm 0.0003$ for the charged pion coupling constant and $f^2 = 0.0745 \pm 0.0006$ for the neutral pion. Ericson *et al.* [57] find from the analysis of np charge-exchange data, $f^2 = 0.0808 \pm 0.0017$.

While results here would seem to confirm (perhaps even with smaller errors due to the determination of the scattering lengths directly from the low-energy data) the results of other analyses of pion-nucleon scattering, there is an important caveat which should be mentioned in regard to all of the analyses with the GMO sum rule. It is the isovector scattering length which enters in the GMO relation. As we saw in the previous section, there is a strong indication of an isospin breaking from the comparison of the elastic scattering determination of this amplitude with its determination from charge exchange. If the explanation advanced in Ref. [46] is correct (so that all of the breaking is in the charge-exchange
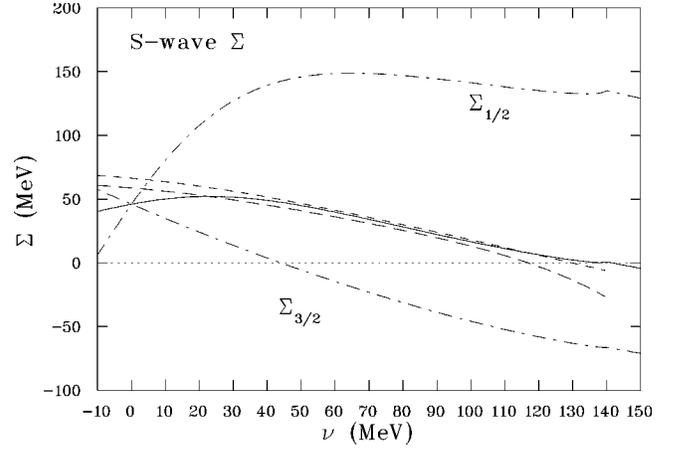

FIG. 8. s wave Σ term amplitude vs ν from the present work (solid curve) compared with the pole-subtracted expansions of Nielsen and Oades [31] (short dash) and Höhler [28] (long dash). The two isospin components from our work are shown with the dash-dot curves.

channel) then the GMO relation will lead to a correct value of f^2. If there is some breaking in the elastic scattering channels then that correction should be made before applying the GMO relation. In the extreme case that all of the breaking comes in the elastic amplitudes (an amplitude of the form of a_3 [47], possibly from ρ-ω mixing, with the opposite sign than predicted) and the isovector amplitude from charge exchange is the correct one, then the pion-nucleon coupling constant would return to the "large" values. It is not possible to reliably determine f^2 (from GMO) until the question of the origin of the isospin breaking is resolved.

D. The Σ term

Figure 8 shows the amplitude defined by Eq. (24) as a function of ν (which is roughly equal to the center-of-mass pion energy ω in this region). Above threshold the real part of the amplitude was used. The result of the solid curve at $\nu = 0$ represents the s-wave contribution to Σ in our model. The solid and dash-dot curves were calculated using the Jost solutions for fit 14 in Table IV. The kinematic singularity at threshold is clearly visible.

While this plot is given as a function of ν, the more relevant variable for extrapolation may be the center-of-mass momentum. Since the CD point lies at $k \approx i\mu$, a circle in the complex plane with radius μ passes through the real axis at a kinetic energy around 57 MeV, or in the center of range studied in this work.

The values obtained for Σ lie around 48 ± 4 MeV. The error quoted is determined from the variation among data sets and does not include the model error. It is interesting to note that there is very little difference between the results from the new π^+ data and that of Bertin *et al.* [10]. This is perhaps understandable from the observation that the Bertin data for the cross section are 20% higher than the prediction from the fits (see Fig. 1) so the $\pi^+ p$ amplitude can be expected to be 10% higher. Since the π^+ and π^- contribute equally to Σ, the difference of the analysis between the two data groups can be expected to be of the order of 5% or 2–3 MeV. Indeed the difference observed is of that order.
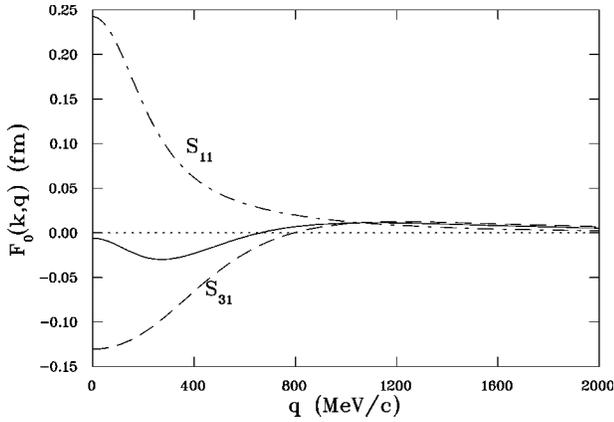
FIG. 9. *s*-wave off-shell amplitudes. The solid line corresponds to the isoscalar combination of the two amplitudes.

While the usually accepted value of Σ is around 65 MeV [22], this is not the first time that a smaller value has been obtained. Ericson found a similar value (44±6 MeV) [24]. If we compare our value of Σ with Σ_d of Ref. [22] (before correction for the $\pi\pi$ channel) we are in good agreement. However, the $\pi\pi$ channel is implicitly included in the present analysis since an integral over the discontinuity of the t cut gives the potential. Thus the singularities in t are present in the model and we must consider the value obtained as including this correction.

E. Off-shell amplitudes

A knowledge of the off-shell amplitude is necessary for the treatment of pion-nucleus scattering. An early determination of these amplitudes was made by Landau and Tabakin [58] using the assumption of a separable potential and deducing the form of the off-shell amplitude from the energy dependence of the on-shell amplitude. Since the knowledge of the scattering amplitude was needed in the region where the scattering becomes inelastic, the potentials obtained were complex, not a very satisfactory situation. Londergan, Mc-Voy and Moniz [59] were able to find real functions for the off-shell dependence by considering only the potentials in the elastic channel, including the inelasticity by coupling to one other two-body channel.

In our case, since we are fitting to data only in the elastic region, there is no problem of a complex extension. We can
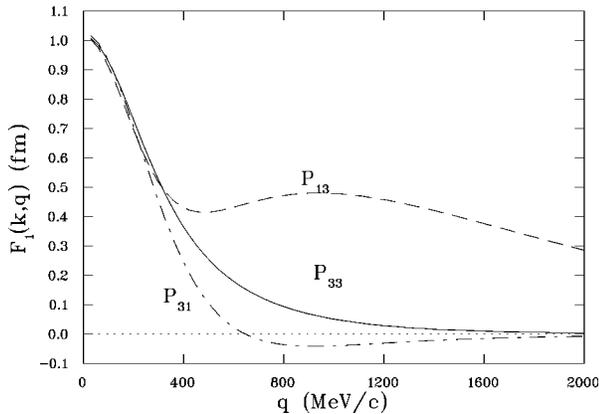

FIG. 10. *p*-wave off-shell amplitudes. Plotted is the ratio of the off-shell value to the on-shell value at 5 MeV.

TABLE VI. Partial total cross sections in mb at the 30° limit.

T_π (MeV)	Present Work	Ref. [64]	Ref. [65]
39.8	7.6		8.5±0.7
44.7	8.9		9.2±0.8
45.0	9.0	10.8± 1.0	
51.7	11.3		11.8±0.8
52.1	11.5	12.4± 1.0	
54.8	12.6		13.2± 0.5
59.3	14.7		15.8± 0.4
63.1	16.6	18.0± 0.6	
66.3	18.4		20.4± 0.4
67.5	19.2	20.7± 0.6	
71.5	21.7	23.8± 0.6	
80.0	28.1		29.7± 0.7
92.5	39.6	43.3± 1.5	

calculate the off-shell amplitudes directly by the Jost formula given in Sec. III for the *s* waves or by direct numerical solution for the *p* waves. Figures 9 and 10 show the ratio of the off-shell amplitudes to the value on-shell at 5 MeV.

Of particular interest is the isoscalar combination of the *s*-wave amplitudes. At low energy this combination nearly vanishes on shell, but this cancellation does not necessarily occur off shell. As can be seen from Fig. 9, for larger values of momentum there is no cancellation at all.

Recent measurements [60] have resulted in accurate threshold cross sections for π^0 production in *pp* collisions. The most common calculation of pion production achieves the needed momentum sharing among the nucleons by rescattering of the meson after it is emitted from one of the protons. Since the *s*-wave $\pi^0 N$ scattering length is near zero, this contribution would seem to be small at threshold. Based on this assumption, Horowitz *et al.* [61] and Lee and Riska [62] constructed models based on heavy-meson exchange which were able to explain the data.

Using the fact that the π^0 is produced ''off-shell,'' Hernández and Oset [63] were able to explain the cross section using an estimated dependence of the off-shell behavior. Their results are uncertain, however, due to a lack of knowledge of this dependence.
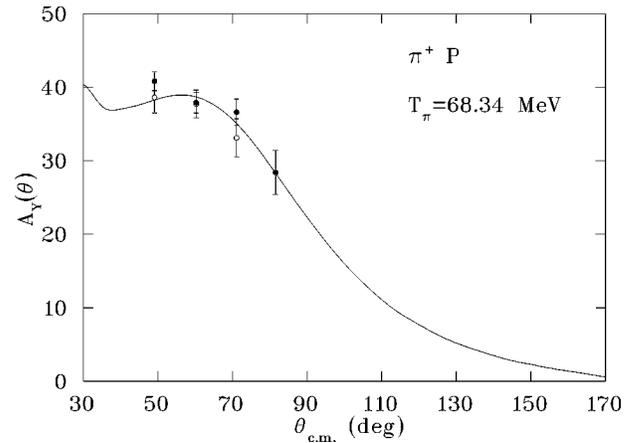

FIG. 11. Comparison of the prediction of the fit with the polarization asymmetry data of Wieser *et al.* [66,67].

TABLE VII. Results of the study with a Gaussian potential with the condition that $\Delta E_\Sigma = 1$ MeV.

		χ^2/N (Data)	χ^2/N (N)	Σ (MeV)	a_3 (μ^{-1})	a_1 (μ^{-1})	f^2	P_{33}	P_{13}	P_{31}	P_{11}
1	Brack	68.25/62	13.45/10	22.59	-0.085	0.174	0.0754	0.168	-0.029	-0.028	-0.061
2	+Frank	231.72/228	26.64/16	22.86	-0.089	0.175	0.0763	0.166	-0.026	-0.026	-0.063
3	+Auld	242.71/239	27.48/17	22.81	-0.089	0.175	0.0763	0.166	-0.026	-0.026	-0.063
4	+Ritchie	272.89/267	31.90/20	22.83	-0.089	0.175	0.0763	0.167	-0.026	-0.025	-0.063
5	+Wiedner	314.50/306	37.36/22	22.89	-0.089	0.175	0.0763	0.166	-0.026	-0.025	-0.063
6	+Joram I	441.25/386	39.86/26	22.86	-0.086	0.173	0.0754	0.167	-0.027	-0.025	-0.064
7	+Joram II	516.30/417	46.08/30	23.14	-0.087	0.173	0.0756	0.166	-0.025	-0.025	-0.064

For the p waves (Fig. 10) it can be seen that the off-shell dependence of the P_{31} and P_{13} (as well as the P_{33}) amplitudes is nearly identical below 300 MeV/c. This fact indicates that the long-range part of the interaction is the same for these three waves.

F. Partial total cross sections

Recently transmission measurements have been made [64,65] to determine the integrated elastic cross section beyond a fixed angle: ''partial total cross sections.'' While many of these measurements were made at higher energies than those treated here, there are several points in the energy region of interest. We have not included these points in the fit but now compare with the values obtained. Until recently the two measurements have differed but now there seems to be general agreement between them, but disagreement with the Brack data above 50 MeV. Our values are shown in Table VI.

G. Polarization asymmetry

While there is no published data on the polarization asymmetry in low-energy charged pion scattering there is one measurement at 68.34 MeV which has appeared in conference proceedings [66] and in a thesis [67]. The prediction of our fits are in excellent agreement with these data as shown in Fig. 11.

H. Gaussian fits

While a Gaussian potential has little theoretical justification, some fits were made with this form to test the sensitivity to the model potential. If a result is stable under this change it may well be believed to be weakly dependent of the form of the potential function. The results are shown in Table VII. It is seen that the values for the pion-nucleon coupling constant remain within a very narrow range, the same range as for the exponential potential, and thus are not sensitive to the potential form chosen.

Another result which is only weakly dependent of the potential form are the scattering volumes of the P_{31} and P_{13} partial waves. They are again found to be equal, albeit slightly smaller than for the exponential case. The values of other scattering volumes are altered significantly, especially the P_{11} wave which is small in this region and hence difficult to determine.

The value of the Σ term is found to vary by less than $\pm 1/2$ MeV over the data sets, but with a different value than for the exponential potential. Thus, in the KG model, the

extrapolation to the CD point depends on the form of the assumed potential.

VI. SUMMARY

We have analyzed recent low-energy pion-proton elastic scattering data. The principal findings are as follows.

(1) The large bulk of the modern elastic scattering data is internally consistent and inconsistent with the older ''Bertin'' data.

(2) The observation of the isospin violation previously indicated was confirmed for the variations in the data set fit over a larger range in energy.

(3) The value of the subthreshold parameter, the Σ term, has been extracted with the exponential potential and the result is a value around 50 MeV, lower than previous estimates. The smallness of this value was shown not to be because of the change in data (which had little effect) but due to the model which was used. This conclusion is reinforced by the study with the Gaussian potential (considered unrealistic) in which a yet smaller value was found.

(4) The pion-nucleon coupling constant was extracted from the scattering lengths with the use of the GMO sum rule and a value ($f^2 = 0.0756 \pm 0.0007$) in agreement with most (but not all) modern determinations was obtained.

(5) Scattering volumes were extracted for the p waves. The parameters for the P_{13} and P_{31} were found to be the same within errors, as predicted from the Chew-Low theory and various improvements [37] and the limit of a large N_c expansion of QCD [40]. The value of the P_{33} scattering volume was found to be smaller than previous determinations.

(6) Off-shell amplitudes for pion-nucleon scattering at low momentum transfers were obtained. The isospin-zero combination of the s-wave amplitudes was shown to be relatively large off shell. Rather remarkably, the P_{13}, P_{31} and P_{33} have the same off-shell dependence for momenta below 300 MeV/c.

[1] W. R. Gibbs, Li Ai, and W. B. Kaufmann, Phys. Rev. Lett. **74**, 3740 (1995); πN Newsletter **2**(11), 84 (1995).

[2] P. B. Sigel and W. R. Gibbs, Phys. Rev. C **33**, 1407 (1986).

[3] Rob G. E. Timmermans, πN Newsletter **2**(11), 7 (1995).

[4] E. J. O. Gavin, R. M. Adam, H. Fiedeldey, and S. A. Sofianos, Few-Body Syst. **19**, 59 (1995).

[5] D. Sigg *et al.*, Phys. Rev. Lett. **75**, 3245 (1995); W. Beer *et al.*, Phys. Lett. B **261**, 16 (1991).

[6] J. T. Brack *et al.*, Phys. Rev. C **41**, 2202 (1990). At 66.8 MeV the 6 largest-angle points for π^+ were replaced with those from Ref. [7] and the smallest angle point was rejected in the π^- data set.

[7] J. T. Brack *et al.*, Phys. Rev. C **38**, 2427 (1988).

[8] J. T. Brack *et al.*, Phys. Rev. C **34**, 1771 (1986). The 66.8 MeV π^+ data from Ref. [7] was used instead of the data from this reference. At the same energy the point at 127.5° was rejected in the π^- data set.

[9] J. S. Frank *et al.*, Phys. Rev. D **28**, 1569 (1983).

[10] P. Y. Bertin *et al.*, Nucl. Phys. **B106**, 341 (1976).

[11] E. G. Auld *et al.*, Can. J. Phys. **57**, 73 (1979).

[12] B. Ritchie *et al.*, Phys. Lett. **125B**, 128 (1983).

[13] U. Wiedner *et al.*, Phys. Rev. D **40**, 3568 (1989); Phys. Rev. Lett. **58**, 648 (1987).

[14] Ch. Joram *et al.*, Phys. Rev. C **51**, 2144 (1995).

[15] Ch. Joram *et al.*, Phys. Rev. C **51**, 2159 (1995).

[16] G. Höhler and H. M. Staudenmaier, πN Newsletter **2**(11), 194 (1995).

[17] R. Jost, Helv. Chim Acta **20**, 256 (1947).

[18] G. Höhler, edited by H. Schopper, Landolt-Börnstein, New Series, Group I, Vol. 9, b2 (Springer-Verlag, Berlin, 1983), p. A.6.49.

[19] D. K. Campbell, *Physics with Heavy Ions and Mesons*, Les Houches (North-Holland, Amsterdam, 1977), p. 549.

[20] R. Koch, Z. Phys. C **15**, 161 (1982).

[21] D. Moir, R. Jacob, and G. Hite, Nucl. Phys. **B103**, 447 (1976).

[22] M. Sainio, πN Newsletter **10**, 13 (1995).

[23] T. P. Cheng and R. Dashen, Phys. Rev. Lett. **26**, 594 (1971).

[24] T. E. O. Ericson, Phys. Lett. B **195**, 116 (1987).

[25] G. Höhler, *Chiral Dynamics: Theory and Experiment Workshop*, 1994, MIT, Vol. 452 of *Lecture Notes in Physics*, edited by A. M. Bernstein and B. R. Holstein (Springer-Verlag, Berlin, 1995), p. 199.

[26] B. Tromborg, S. Waldenstrom, and I. Overbo, Helv. Chim Acta **51**, 584 (1978).

[27] L. D. Roper, R. M. Wright, and B. T. Feld, Phys. Rev. **138**, B190 (1965).

[28] *Handbook of Pion-Nucleon Scattering*, edited by G. Höhler, F. Kaiser, R. Koch, and E. Pietarinen (Institut für Theoretische Kernphysik der Universität Karlsruhe, Germany, 1979).

[29] W. N. Cottingham, M. Lacombe, B. Loiseau, J. M. Richard, and R. Vinh Mau, Phys. Rev. D **8**, 800 (1973); M. Lacombe, B. Loiseau, J. M. Richard, R. Vinh Mau, J. Côté, P. Pirès, and R. de Tourreil, Phys. Rev. C **21**, 861 (1980).

[30] H. Nielsen, Nucl. Phys. **B30**, 317 (1971).

[31] H. Nielsen and G. C. Oades, Nucl. Phys. **B72**, 310 (1974).

[32] L. Brown, W. J. Pardee, and R. D. Peccei, Phys. Rev. D **4**, 2801 (1971).

[33] D. Murphy and S. Coon, Few-Body Syst. **18**, 73 (1995).

[34] E. D. Cooper and B. K. Jennings, Phys. Rev. D **33**, 1509 (1986).

[35] V. Bernard, N. Kaiser, and U.-G. Meissner, Phys. Lett. B **309**, 421 (1993): Phys. Rev. C **52**, 2185 (1995).

[36] E. M. Henley and W. Thirring, *Elementary Quantum Field Theory* (McGraw-Hill, New York, 1962).

[37] T. E. O. Ericson and W. Weise, *Pions and Nuclei* (Clarendon, Oxford, 1988).

[38] E. Oset, H. Toki, and W. Weise, Phys. Rep. **83**, 282 (1982).

[39] Marek Karliner and Michael P. Mattis, in *Intersections Between Particle and Nuclear Physics*, Proceedings of the International Conference, Lake Louise, Canada 1986, AIP Conf. Proc. No. 150, edited by Donald F. Geesaman (AIP, New York, 1986), p. 762; M. P. Mattis and M. Karliner, Phys. Rev. D **31**, 2833 (1985).

[40] R. Dashen and A. V. Manohar, Phys. Lett. B **315**, 425 (1993).

[41] R. Koch and E. Pietarinen, Nucl. Phys. **B336**, 331 (1980).

[42] M. E. Sadler *et al.*, πN Newsletter (5) (1992); J. Duclos *et al.*, Phys. Lett. **43B**, 245 (1973); D. H. Fitzgerald *et al.*, Phys. Rev. C **34**, 619 (1985); M. E. Sadler (private communication); SAID interactive dial-in program (unpublished).

[43] M. Salomon *et al.*, Nucl. Phys. **A414**, 493 (1984).

[44] A. Bagheri *et al.*, Phys. Rev. C **38**, 885 (1988).

[45] B. L. Birbriar and A. B. Gridnov, Phys. Lett. B **335**, 6 (1994).

[46] J. Piekarewicz, Phys. Lett. B **358**, 27 (1995).

[47] W. B. Kaufmann and W. R. Gibbs, Ann. Phys. (N.Y.) **214**, 84 (1992).

[48] M. L. Goldberger, H. Miyazawa, and R. Oehme, Phys. Rev. **99**, 986 (1955); see also Ref. [18].

[49] R. L. Workman, R. A. Arndt, and M. M. Pavan, Phys. Rev. Lett. **68**, 1653 (1992): **68**, 2712(E) (1992).

[50] R. A. Arndt and R. Roper, SAID dial-in program [42].

[51] Particle Data Group, Phys. Rev. D **50**, 1173 (1994).

[52] R. A. Arndt, I. I. Strakovsky, R. Workman, and M. M. Pavan, Phys. Rev. C **52**, 2120 (1995).

[53] M. Locher and M. Sainio, *XIII International Conference on Particles and Nuclei*, Perugia, 1993 (unpublished).

[54] R. A. Arndt, R. L. Workman, and M. M. Pavan, Phys. Rev. C **49**, 2729 (1994).

[55] F. G. Markopoulou-Kalamara and D. V. Bugg, Phys. Lett. B **318**, 565 (1993).

[56] R. A. M. Klomp *et al.*, Phys. Rev. C **44**, R1258 (1991); V. Stoks *et al.*, *ibid.* **47**, 512 (1993).

[57] T. E. O. Ericson, B. Loiseau, J. Nilsson, N. Olsson, J. Blomgren, H. Condé, K. Elmgren, O. Johnsson, L. Nilsson, P.-U. Renberg, A. Ringbom, T. Rönnqvist, G. Tibell, and R. Zorro, Phys. Rev. Lett. **75**, 1046 (1995); T. E. O. Ericson, B. Loiseau, J. Nilsson, and N. Olsson, Few-Body Syst., Suppl. **8**, 254 (1995).

[58] R. Landau and F. Tabakin, Phys. Rev. D **5**, 2746 (1972).

[59] J. T. Londergan, K. W. McVoy, and E. J. Moniz, Ann. Phys. (N.Y.) **86**, 147 (1974).

[60] H. O. Meyer *et al.*, Nucl. Phys. **A539**, 633 (1992).

[61] C. J. Horowitz, H. O. Meyer, and D. K. Griegel, Phys. Rev. C **49**, 1337 (1994).

[62] T-S. H. Lee and D. O. Riska, Phys. Rev. Lett. **70**, 2237 (1993).

[63] E. Hernández and E. Oset, Phys. Lett. B **350**, 158 (1995).

[64] E. Friedman *et al.*, Nucl. Phys. **A514**, 601 (1990) [corrected values are given in M. M. Pavan, πN Newsletter **11**, 117 (1995)].

[65] B. J. Kriss *et al.*, πN Newsletter **8**, 1 (1993); R. A. Ristinen, *ibid.* **11**, 1 (1995); B. J. Kriss *et al.*, in *Proceedings of the 5th International Symposium on Meson-Nucleon Physics and the Structure of the Nucleon*, Boulder, 1993, edited by G. Hoehler, W. Kluge, and B. M. K. Nefkens (unpublished), Vol. 1, p. 17.

[66] R. Wieser *et al.*, in *Proceedings of the Blaubeuren/Tübingen Meeting* [πN Newletter **1**(10), 125 (1995)].

[67] R. Wieser *et al.*, Phys. Rev. C **54**, 1930 (1996); R. Wieser, Ph.D. thesis, University of Karlsruhe, 1995 (unpublished).